

Ergodic Spectral Efficiency of Massive MIMO with Correlated Rician Channel and MRC Detection based on LS and MMSE Channel Estimation

Mohammad Hadi Sadraei ¹ Mohammad Sadegh Fazel ² Ali Mohamad Doost-Hoseini ³

¹ Department of Electrical and Computer Engineering, Isfahan University of Technology, Isfahan 84156 83111, Iran* E-mail: mh.sadraei@ec.iut.ac.ir

² Department of Electrical and Computer Engineering, Isfahan University of Technology, Isfahan 84156 83111, Iran* E-mail: fazel@cc.iut.ac.ir

³ Department of Electrical and Computer Engineering, Isfahan University of Technology, Isfahan 84156 83111, Iran* E-mail: alimdh@cc.iut.ac.ir

ISSN 1751-8644
doi: 0000000000
www.ietdl.org

Abstract: In this paper, we study the spectral efficiency (SE) of a multi-cell massive multiple-input multiple-output (MIMO) system with a spatially correlated Rician channel. The correlation between least squares (LS) estimator and its error complicates SE analysis, since signal and interference components become cross-correlated, too. Minimum mean square error (MMSE) estimators do not suffer from this burden. In some previous works, a proper part of the signal is referred to interference, which makes them cross-uncorrelated, and leads to an SE lower bound. In our modified approach, we extract and refer the cross-correlated part of interference to the signal to attain this objective. Here, we use this approach for calculating the instantaneous SE of maximum ratio combining (MRC) detector under LS and MMSE estimation methods. We also derive closed-form approximations of their ergodic SE. This approach is also applicable to other linear channel estimators or data detectors. Numerical results show that achievable SE surpasses that of the previous approach. They also show that our approximation is close enough to Monte Carlo simulation results, especially at the high number of the base station (BS) antennas.

Index terms: Massive MIMO, Uplink, Spectral Efficiency, LS Channel Estimation, MMSE Channel Estimation

1 Introduction

Higher SE with reliable transmission is an obvious requirement in wireless communication systems, since the available spectrum is saturated [1]. Massive MIMO system is one of the solutions for improving SE [2]. In this system, the BS in each cell is equipped with a large number of antennas compared to active users [3]. Cross-interference and uplink thermal noise vanish by a high increase in the number of BS antennas, as a result of random matrix properties [4, 5]. Moreover, linear processing at BS can provide an achievable sum-rate close to optimal non-linear solutions like maximum likelihood (ML) detection in uplink and dirty paper coding (DPC) in downlink [6].

SE of massive MIMO systems has been mostly investigated for uncorrelated Rayleigh channel in both uplink [7–14] and downlink [14–16]. Among these works, the single-cell scenario is assumed in [8, 9, 11, 12, 15] and multi-cell in [7, 10, 13, 14, 16]. SE of MRC detection is investigated for three cases: perfect channel state information (CSI) [8]; LS [7] and MMSE channel estimation [7–9]. SE of zero forcing (ZF) detector is studied for perfect CSI [8] as well as MMSE channel estimation [8–10]. SE of MMSE detection is evaluated in [8] for both perfect CSI and MMSE channel estimation cases. SE of ML detector is approximated for a multi-cell system in [12] under perfect CSI assumption. In [13], ZF detection is modified to have less inter-cell interference and as a result, higher SE in the presence of MMSE channel estimation.

In [14], both uplink and downlink SE of MRC/MRT and ZF processing at BS are studied for uncorrelated Rayleigh channel with MMSE channel estimation. Lower bounds for SE of maximum ratio transmission (MRT) and ZF pre-coders are provided for MMSE channel estimation in [15]. Achievable SE of MRT and ZF pre-coders are provided in [16] whether with or without downlink pilots.

Correlated Rayleigh channel is also considered for single-cell [17] and multi-cell systems [18]. In a more practical case for correlated

Rayleigh channel, the effect of covariance estimation error on both uplink and downlink SE of MMSE channel estimation is studied in [18]. In [17], ZF pre-coding is modified to achieve higher SE of the perfect CSI case for a correlated Rayleigh channel.

1.1 Related Literature

When there is a strong line of sight (LOS) component between users and BS, the transmission channel exhibits a Rician model. SE approximations of massive MIMO Rician channels are provided in [19–22] for the uplink including MRC [20–22] and ZF detector [19]; and [21–24] for the downlink covering MRT [21–23] and ZF pre-coder [24]. However, spatial correlation is considered only in [20, 22]. Perfect CSI is assumed in [20] while in [22] non-ideal LS and MMSE channel estimations are taken into account. Imperfect CSI is also considered in [23], but for uncorrelated Rician channel. In [22, 23], a multi-cell system is considered, while in the other mentioned works single-cell scenario is studied.

1.2 Contribution

To the best of our knowledge, SE analysis for correlated Rician channel and imperfect CSI is presented only in [22]. In their work, the authors consider the mean inner product of the detector and channel vectors as the desired channel response for each user. By this assumption, signal and interference decorrelate at the detector output. However, as less of the available CSI is used, the effective SINR is less than its real value. In our work, the inner product of channel estimate and detector vectors is considered as equivalent channel response for each user. Hence, all available CSI is used. However, signal and interference are not necessarily cross-uncorrelated, which makes SE analysis more difficult. We overcome this difficulty by extracting the correlated component of interference with the signal and adding it to the desired signal part. Thus, modified desired signal and interference become cross-uncorrelated to afford instantaneous

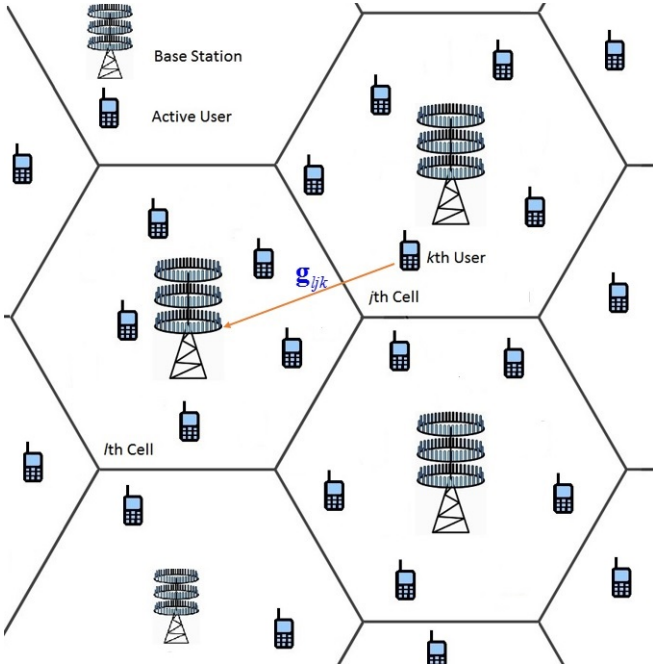


Fig. 1: Multi-cell massive MIMO scenario and the channel between k th user in j th cell and BS in l th cell

SE calculation. Besides, some near-optimal closed-form formulas are also derived for ergodic SE. To sum up, the main contributions of this paper are as follows:

- In a multi-cell correlated Rician channel, we propose to extract all data-dependent components at the detector output as a signal. Therefore instantaneous SE can be calculated in the form of $\log_2(1 + \text{SINR})$.
- An approximation is proposed for closed-form ergodic SE. Necessary statistics are also derived by using quadratic and quartic moments of a complex normal vector. These are derived by using sufficient statistics of MMSE and LS estimators.
- We compare our proposed approximation with Monte Carlo simulation results as well as [22] for both single-cell and multi-cell correlated Rician channels. Moreover, we show the superiority of our work and the closeness of the proposed approximation to simulation results.

1.3 Outline

The rest of the paper is organized as follows: In Section 2 system model, pilot and data transmission processes are discussed. We propose our SE analysis and also ergodic SE approximation in Section 3. Numerical results are provided in Section 4. Finally, the paper is concluded in Section 5.

1.4 Notation

Vectors and matrices are boldface lower and higher cases, respectively. Superscript $(\cdot)^H$ denotes complex conjugate transpose (hermitian) of a vector or matrix. The trace of \mathbf{X} is shown by $\text{Tr}\{\mathbf{X}\}$. Symbols $\mathbb{E}[\mathbf{x}]$ and $\|\mathbf{x}\|$ denote the expected value and Frobenius norm of \mathbf{x} , respectively. Set of all complex matrices with $K \times M$ size and vectors with K elements are denoted by $\mathbb{C}^{K \times M}$ and \mathbb{C}^K , respectively. The identity matrix is indicated by \mathbf{I} . Complex normal vector with mean \mathbf{m} and covariance matrix Σ is shown by $\mathcal{CN}(\mathbf{m}, \Sigma)$.

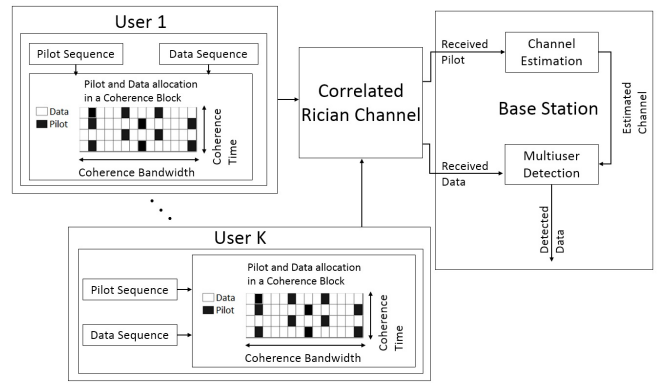


Fig. 2: Block diagram of pilot and data allocation at users; channel estimation and data detection at BS over one coherence block

2 System Model

We consider the uplink of a system with L cells (Fig. 1), where each BS contains M antennas and serves K single-antenna users. Orthogonal frequency division multiplexing (OFDM) is used such that no inter-symbol-interferences and inter-carrier-interferences exist. Within each coherence block, the channel between k th user in j th cell and BS in l th cell is described as vector $\mathbf{g}_{ljk} \in \mathbb{C}^M$ which has a $\mathcal{CN}(\mathbf{m}_{ljk}, \mathbf{R}_{ljk})$ distribution. Thus, the magnitudes of elements of \mathbf{g}_{ljk} have a Rician distribution. Non-zero off-diagonal elements of \mathbf{R}_{ljk} represent channel spatial correlation. The channel vectors are assumed to be independent for different values of (l, j, k) because users are distributed widely in each cell. The mean vectors (\mathbf{m}_{ljk}) correspond to the LOS components and depend on the large scale fading factors (β_{ljk}^{LOS}) . The covariance matrices (\mathbf{R}_{ljk}) are related to non-LOS paths and depend on their large scale fading multiples (β_{ljk}^{NLOS}) .

As seen in Fig. 2, for each block, BS estimates the channel and detects the data. Channel estimation is done by processing the received pilot sequences. Data detection is done by using the estimated channel.

2.1 Channel Estimation

We assume that k th user in l th cell transmits the pilot sequence $\sqrt{q_{lk}}\boldsymbol{\phi}_k$ of length τ_p , where q_{lk} is symbol power and $\boldsymbol{\phi}_k$ is such that $\|\boldsymbol{\phi}_k\|^2 = \tau_p$. By assuming $\tau_p \geq K$, we can have mutually orthogonal sequences. We restrict our analysis only to the l th cell. For simplicity the index l is dropped in \mathbf{g}_{lk} , \mathbf{m}_{lk} , \mathbf{R}_{lk} and they are expressed as \mathbf{g}_k , \mathbf{m}_k , \mathbf{R}_k , respectively. The received pilot signals at BS are denoted by matrix $\mathbf{\Psi} \in \mathbb{C}^{M \times \tau_p}$ such that

$$\mathbf{\Psi} = \sum_{j=1}^L \sum_{i=1}^K \sqrt{q_{ji}} \mathbf{g}_{lji} \boldsymbol{\phi}_i + \mathbf{W} \quad (1)$$

where $\mathbf{W} \in \mathbb{C}^{M \times \tau_p}$ is the additive white Gaussian noise (AWGN) matrix with i.i.d $\mathcal{CN}(0, \sigma_n^2)$ entries. At BS, the product $\mathbf{\Psi} \boldsymbol{\phi}_k^H$ possesses sufficient statistics for estimating \mathbf{g}_k :

$$\mathbf{\Psi} \boldsymbol{\phi}_k^H = \tau_p \sum_{j=1}^L \sqrt{q_{jk}} \mathbf{g}_{ljk} + \mathbf{W} \boldsymbol{\phi}_k^H \quad (2)$$

The vector $\mathbf{\Psi} \boldsymbol{\phi}_k^H$ is the sum of independent complex normal vectors and consequently is a complex normal vector, too. In the following this vector is used in both LS and MMSE estimation.

2.1.1 LS Method: By considering the orthogonality property of pilot sequences [25], LS estimate of \mathbf{g}_k is written as

$$\hat{\mathbf{g}}_k^{ls} = \frac{1}{\tau_p \sqrt{q_{lk}}} \mathbf{\Psi} \boldsymbol{\phi}_k^H = \mathbf{g}_k + \sum_{j \neq l} \sqrt{\frac{q_{jk}}{q_{lk}}} \mathbf{g}_{ljk} + \frac{1}{\tau_p \sqrt{q_{lk}}} \mathbf{W} \boldsymbol{\phi}_k^H \quad (3)$$

Hence, the estimate \hat{g}_k^{ls} has $\mathbb{C}N(\mathbf{h}_k, \mathbf{S}_k)$ distribution where its mean vector (\mathbf{h}_k) and covariance matrix (\mathbf{S}_k) are:

$$\mathbf{h}_k = \mathbf{m}_k + \sum_{j \neq l} \sqrt{\frac{q_{jk}}{q_{lk}}} \mathbf{m}_{ljk} \quad (4)$$

$$\mathbf{S}_k = \mathbf{R}_k + \sum_{j \neq l} \frac{q_{jk}}{q_{lk}} \mathbf{R}_{ljk} + \frac{\sigma_n^2}{\tau_p q_{lk}} \mathbf{I} \quad (5)$$

Proof: The vector \hat{g}_k^{ls} is a sum of independent complex normal vectors and has a complex normal distribution. Its mean is derived simply by taking the expectation of the right side of (3). Finally, since all the terms on the right side are cross-uncorrelated, their covariance summation equals \mathbf{S}_k . \square

If the LS channel estimator error (\tilde{g}_k^{ls}) is defined by $\tilde{g}_k^{ls} \triangleq \mathbf{g}_k - \hat{g}_k^{ls}$ then by similar reasoning, it has $\mathbb{C}N(\bar{\mathbf{h}}_k, \mathbf{T}_k)$ distribution, where its mean vector ($\bar{\mathbf{h}}_k$) and covariance matrix (\mathbf{T}_k) are as follows:

$$\bar{\mathbf{h}}_k = \mathbf{m}_k - \mathbf{h}_k = - \sum_{j \neq l} \sqrt{\frac{q_{jk}}{q_{lk}}} \mathbf{m}_{ljk} \quad (6)$$

$$\mathbf{T}_k = \sum_{j \neq l} \frac{q_{jk}}{q_{lk}} \mathbf{R}_{ljk} + \frac{\sigma_n^2}{\tau_p q_{lk}} \mathbf{I} \quad (7)$$

According to (6) LS estimation in equation (3) is biased unless $\mathbf{m}_{ljk} = 0$ for all $j \neq l$. The estimated channel is considered as the true channel response and its error is incorporated into interference and noise terms. According to equation (3), the vectors \hat{g}_k^{ls} and \tilde{g}_k^{ls} are correlated with cross-covariance matrix $-\mathbf{T}_k$. The effect of this cross-correlation on data detection will be discussed in Section 3.

2.1.2 MMSE Method: The MMSE estimation of \mathbf{g}_k [25] is

$$\hat{g}_k^m = \tau_p \sqrt{q_{lk}} \mathbf{R}_k \boldsymbol{\Omega}_k^{-1} \left(\boldsymbol{\Psi} \boldsymbol{\phi}_k^H - \tau_p \sum_{j=1}^L \sqrt{q_{jk}} \mathbf{m}_{ljk} \right) + \mathbf{m}_k \quad (8)$$

where

$$\boldsymbol{\Omega}_k = \tau_p^2 \sum_{j=1}^L q_{jk} \mathbf{R}_{ljk} + \sigma_n^2 \tau_p \mathbf{I}. \quad (9)$$

The estimation \hat{g}_k^m and its error (i.e., $\tilde{g}_k^m \triangleq \mathbf{g}_k - \hat{g}_k^m$) are distributed as

$$\hat{g}_k^m \sim \mathbb{C}N(\mathbf{m}_k, \mathbf{U}_k) \quad (10)$$

$$\tilde{g}_k^m \sim \mathbb{C}N(\mathbf{0}, \mathbf{V}_k) \quad (11)$$

where their covariance matrices are equal to:

$$\mathbf{U}_k = \mathbf{R}_k \mathbf{S}_k^{-1} \mathbf{R}_k \quad (12)$$

$$\mathbf{V}_k = \mathbf{R}_k - \mathbf{U}_k \quad (13)$$

Proof: According to (8), the vectors \hat{g}_k^m and $\boldsymbol{\Psi} \boldsymbol{\phi}_k^H$ have an affine relation. Since $\boldsymbol{\Psi} \boldsymbol{\phi}_k^H$ is a complex normal vector and \hat{g}_k^m is either. It is clear that MMSE estimation is unbiased, hence $E[\hat{g}_k^m] = E[\mathbf{g}_k]$ and $E[\tilde{g}_k^m] = 0$. The covariance of \hat{g}_k^m (i.e., \mathbf{U}_k) is derived by multiplying $\tau_p \sqrt{q_{lk}} \mathbf{R}_k \boldsymbol{\Omega}_k^{-1}$ and its hermitian to left and the right side of $\boldsymbol{\Omega}_k$, respectively. This leads to $\mathbf{U}_k = \tau_p^2 q_{lk} \mathbf{R}_k \boldsymbol{\Omega}_k^{-1} \mathbf{R}_k$. From (5), it is concluded that $\boldsymbol{\Omega}_k = \tau_p^2 q_{lk} \mathbf{S}_k$ and the proof of equation (12) is now complete. From the orthogonality of MMSE estimator and its error: $E[\tilde{g}_k^m (\tilde{g}_k^m)^H] = (E[\mathbf{g}_k \mathbf{g}_k^H] - \mathbf{m}_k \mathbf{m}_k^H) - (E[\hat{g}_k^m (\hat{g}_k^m)^H] - \mathbf{m}_k \mathbf{m}_k^H)$. By direct substitution, equation (13) is derived. \square

2.2 Multi-user Data Detection

We assume that each user sends its data vector using the same τ_u time-frequency resource. For simplicity, only one of these resources is considered. In the data transmission phase, $\mathbf{x}_j \in \mathbb{C}^K$ is transmitted by users in the j th cell such that $E[\mathbf{x}_j \mathbf{x}_j^H] = \mathbf{P}_j$, where \mathbf{P}_j is a diagonal matrix which consists of users' average powers. The received data at the l th BS (i.e., $\mathbf{y} \in \mathbb{C}^M$) is as follows:

$$\mathbf{y} = \sum_{i=1}^K \mathbf{g}_i \mathbf{x}_{li} + \sum_{j \neq l} \sum_{i=1}^K \mathbf{g}_{lji} \mathbf{x}_{ji} + \mathbf{n} \quad (14)$$

where \mathbf{x}_{ji} is the data symbol transmitted by i th user in j th cell and $\mathbf{n} \in \mathbb{C}^M$ describes the noise vector consisting of i.i.d $\mathbb{C}N(0, \sigma_n^2)$ elements. In MRC detector, the received vector (\mathbf{y}) is multiplied by $\hat{\mathbf{g}}_k^H$. Thus, the detected signal of k th user in the l th cell (\hat{x}_{lk}) is represented by:

$$\begin{aligned} \hat{x}_{lk} = & \hat{\mathbf{g}}_k^H \hat{\mathbf{g}}_k \mathbf{x}_{lk} + \sum_{i=1}^K \hat{\mathbf{g}}_k^H \tilde{\mathbf{g}}_i \mathbf{x}_{li} + \sum_{i \neq k} \hat{\mathbf{g}}_k^H \hat{\mathbf{g}}_i \mathbf{x}_{li} \\ & + \sum_{j \neq l} \sum_{i=1}^K \hat{\mathbf{g}}_k^H \mathbf{g}_{lji} \mathbf{x}_{ji} + \hat{\mathbf{g}}_k^H \mathbf{n}. \end{aligned} \quad (15)$$

The detected data \hat{x}_{lk} includes five terms. Among these terms, only the first one is desirable. The second term corresponds to channel estimation error. The third and fourth terms are intra-cell and inter-cell interferences, respectively. The last one is due to AWGN noise. In the next section, equation (15) is used to calculate SE.

3 Spectral efficiency in presence of LS and MMSE channel estimation

In this section, the calculation of instantaneous SE and approximating its average are discussed. If the desirable term were uncorrelated with others, SE of k th user would be obtained by $\log_2(1 + \text{SINR}_k)$, where SINR_k is simply the power ratio of the desired term to undesired terms. Since the users' data are independent, the only possibly correlated terms are $\hat{\mathbf{g}}_k^H \hat{\mathbf{g}}_k \mathbf{x}_{lk}$ and $\hat{\mathbf{g}}_k^H \tilde{\mathbf{g}}_k \mathbf{x}_{lk}$. The vectors $\hat{\mathbf{g}}_k$ and $\tilde{\mathbf{g}}_k$ are not necessarily cross-uncorrelated if MMSE channel estimation is not used. As a result, signal and interference are dependent, and their SE analysis is much difficult. The cross-correlated part of interference is incorporated into the signal. By extracting $\hat{\mathbf{g}}_k^H \hat{\mathbf{g}}_k$ (linear MMSE estimation of $\tilde{\mathbf{g}}_k$ given $\hat{\mathbf{g}}_k$) from $\tilde{\mathbf{g}}_k$, $\bar{\mathbf{g}}_k \triangleq \tilde{\mathbf{g}}_k - \hat{\mathbf{g}}_k^H \hat{\mathbf{g}}_k \tilde{\mathbf{g}}_k$ is uncorrelated with $\hat{\mathbf{g}}_k$. Then, $\hat{\mathbf{g}}_k + \hat{\mathbf{g}}_k^H \hat{\mathbf{g}}_k \tilde{\mathbf{g}}_k = \hat{\mathbf{g}}_k$, $\bar{\mathbf{g}}_k = \tilde{\mathbf{g}}_k$, and equation (15) can be rewritten as:

$$\begin{aligned} \hat{x}_k = & \hat{\mathbf{g}}_k^H \hat{\mathbf{g}}_k^m \mathbf{x}_{lk} + \sum_{i=1, i \neq k}^K \hat{\mathbf{g}}_k^H \hat{\mathbf{g}}_i^m \mathbf{x}_{li} + \sum_{i=1}^K \hat{\mathbf{g}}_k^H \tilde{\mathbf{g}}_i^m \mathbf{x}_{li} \\ & + \sum_{j \neq l} \sum_{i=1}^K \hat{\mathbf{g}}_k^H \mathbf{g}_{lji} \mathbf{x}_{ji} + \hat{\mathbf{g}}_k^H \mathbf{n} \end{aligned} \quad (16)$$

The term $\hat{\mathbf{g}}_k^H \hat{\mathbf{g}}_k^m \mathbf{x}_{lk}$ is uncorrelated with others. Thus, the power of all expressions in (16) over a coherence block can be used for calculating instantaneous SE of k th user (η_k). In calculating these powers, only $\hat{\mathbf{g}}_k$ and $\hat{\mathbf{g}}_k^m$ are deterministic. For any linear channel estimator, SE is expressed as

$$\eta_k = \gamma \log_2 \left(1 + \frac{p_{lk} |\hat{\mathbf{g}}_k^H \hat{\mathbf{g}}_k^m|^2}{I_1 + I_2 + I_3 + I_4} \right) \quad (17)$$

where the factor γ equals the length ratio of uplink data to coherence block:

$$\gamma = \frac{\tau_u}{\tau_u + \tau_p} \quad (18)$$

The power of $\hat{\mathbf{g}}_k^H \hat{\mathbf{g}}_k^m x_{lk}$ is $p_{lk} |\hat{\mathbf{g}}_k^H \hat{\mathbf{g}}_k^m|^2$. The term I_1 is the power of $\sum_{i=1, i \neq k}^K \hat{\mathbf{g}}_k^H \hat{\mathbf{g}}_i^m x_{li}$ and is equal to

$$I_1 = \sum_{i \neq k} p_{li} |\hat{\mathbf{g}}_k^H \hat{\mathbf{g}}_i^m|^2 \quad (19)$$

I_2 corresponds to the power of $\sum_{i=1}^K \hat{\mathbf{g}}_i^H \hat{\mathbf{g}}_i^m x_{li}$ and is written as

$$I_2 = \hat{\mathbf{g}}_k^H \left(\sum_{i=1}^K p_{li} \mathbf{V}_i \right) \hat{\mathbf{g}}_k \quad (20)$$

The power of $\sum_{j \neq l} \sum_{i=1}^K \hat{\mathbf{g}}_k^H \mathbf{g}_{lji} x_{ji}$ is equal to

$$I_3 = \hat{\mathbf{g}}_k^H \left(\sum_{j \neq l} \sum_{i=1}^K p_{ji} \left(\mathbf{R}_{lji} + \mathbf{m}_{lji} \mathbf{m}_{lji}^H \right) \right) \hat{\mathbf{g}}_k \quad (21)$$

And the term I_4 is the power in $\hat{\mathbf{g}}_k^H \mathbf{n}$:

$$I_4 = \sigma_n^2 \|\hat{\mathbf{g}}_k\|^2. \quad (22)$$

The ergodic SE is obtained by averaging (17) over all possible channel realizations. Unfortunately, an exact closed-form average is not accessible. We propose an approximate closed-form using the following lemma.

Lemma 1. If x and y are sums of non-negative random variables, then [26]

$$\mathbb{E} \left[\log \left(1 + \frac{x}{y} \right) \right] \approx \log \left(1 + \frac{\mathbb{E}[x]}{\mathbb{E}[y]} \right) \quad (23)$$

It is shown in [26] that both sides of above approximation have the same lower and also upper bounds. By increasing the number of non-negative random variables, these bounds tighten and the approximation becomes more reliable.

Hence,

$$\mathbb{E}[\eta_k] \approx \bar{\eta}_k = \gamma \log_2 \left(1 + \frac{p_{lk} \mathbb{E} \left[|\hat{\mathbf{g}}_k^H \hat{\mathbf{g}}_k^m|^2 \right]}{\mathbb{E} \left[I_1 + I_2 + I_3 + I_4 \right]} \right) \quad (24)$$

In [22] $p_{lk} \mathbb{E}[\hat{\mathbf{g}}_k^H \mathbf{g}_k]^2$ which equals $p_{lk} \mathbb{E}[\hat{\mathbf{g}}_k^H \hat{\mathbf{g}}_k^m]^2$ is assumed as the signal power, while in (24) the numerator is $p_{lk} \mathbb{E}[\hat{\mathbf{g}}_k^H \hat{\mathbf{g}}_k^m]^2$. As $\mathbb{E}[\hat{\mathbf{g}}_k^H \hat{\mathbf{g}}_k^m]^2 \geq \mathbb{E}[\hat{\mathbf{g}}_k^H \hat{\mathbf{g}}_k^m]^2$, SINR_k in (24) has larger numerator, as well as, smaller denominator compared to that in [22] since they sum up to the detector output power for both works. Therefore, it is concluded that more accurate ergodic SE can be achieved in our approach. In the following, we compute expectations in (24) for MMSE and LS estimators.

3.1 Ergodic spectral efficiency in presence of MMSE channel estimation

In this case, either (15) or (16) can be used for calculating SINR_k, because $\hat{\mathbf{g}}_k | \hat{\mathbf{g}}_k = \mathbf{0}$. If $\hat{\mathbf{g}}_k$ is replaced by $\hat{\mathbf{g}}_k^m$ in (24), then the numerator becomes

$$\mathbb{E} \left[\left\| \hat{\mathbf{g}}_k^m \right\|^4 \right] = \text{Tr} \left\{ \mathbf{U}_k^2 \right\} + 2 \mathbf{m}_k^H \mathbf{U}_k \mathbf{m}_k + \left(\text{Tr} \left\{ \mathbf{U}_k \right\} + \|\mathbf{m}_k\|^2 \right)^2 \quad (25)$$

Proof: Substitute $\mathbf{x} = \hat{\mathbf{g}}_k^m$, $\mathbf{m} = \mathbf{m}_k$ and $\Sigma = \mathbf{U}_k$ in equation (50) of Appendix 7.2. \square

If we denote the means of I_1 , I_2 , I_3 and I_4 over all possible realizations of the channel by I_1^m , I_2^m , I_3^m and I_4^m respectively:

1.

$$I_1^m = \sum_{i \neq k} p_{li} \text{Tr} \left\{ \left(\mathbf{U}_k + \mathbf{m}_k \mathbf{m}_k^H \right) \left(\mathbf{U}_i + \mathbf{m}_i \mathbf{m}_i^H \right) \right\} \quad (26)$$

Proof: Equation (26) is derived by using the trace properties in Appendix 7.3. \square

2.

$$I_2^m = \sum_{i=1}^K p_{li} \text{Tr} \left\{ \mathbf{V}_i \left(\mathbf{U}_k + \mathbf{m}_{lji} \mathbf{m}_{lji}^H \right) \right\} \quad (27)$$

Proof: For calculating $\mathbb{E}[I_2]$, $\mathbb{E}[(\hat{\mathbf{g}}_k^m)^H \mathbf{V}_i \hat{\mathbf{g}}_k^m]$ needs to be derived for a specific i . This is done by using Lemma 2 in Appendix 7.1 with $\mathbf{x} = \hat{\mathbf{g}}_k^m$, $\mathbf{m} = \mathbf{m}_k$, $\Sigma = \mathbf{U}_k$ and $A = \mathbf{V}_i$ substitution. Finally, equation (27) is derived by inserting $\mathbb{E}[(\hat{\mathbf{g}}_k^m)^H \mathbf{V}_i \hat{\mathbf{g}}_k^m]$ in $\mathbb{E}[I_2]$. \square

3.

$$I_3^m = \sum_{j \neq l} \sum_{i=1}^K p_{ji} \text{Tr} \left\{ \left(\mathbf{R}_{lji} + \mathbf{m}_{lji} \mathbf{m}_{lji}^H \right) \left(\mathbf{U}_k + \mathbf{m}_k \mathbf{m}_k^H \right) \right\} \quad (28)$$

Proof: It is similar to equation (27) proof, except that for the double summation. Hence, the inner expectation is derived for specific i and j by replacing $A = \mathbf{R}_{lji} + \mathbf{m}_{lji} \mathbf{m}_{lji}^H$. \square

4.

$$I_4^m = \sigma_n^2 \left(\text{Tr} \left\{ \mathbf{U}_k \right\} + \|\mathbf{m}_k\|^2 \right). \quad (29)$$

Proof: From equation (47) in Appendix 7.1, we have $\mathbb{E}[\|\hat{\mathbf{g}}_k^m\|^2] = \text{Tr}\{\mathbf{U}_k\} + \|\mathbf{m}_k\|^2$, which leads to equation (29). \square

Therefore, the approximate ergodic SE of the k th user ($\bar{\eta}_k^{\text{mmse}}$) in presence of MMSE channel estimation is expressed as

$$\bar{\eta}_k^{\text{mmse}} = \gamma \log_2 \left(1 + \frac{p_{lk} \mathbb{E} \left[\left\| \hat{\mathbf{g}}_k^m \right\|^4 \right]}{I_1^m + I_2^m + I_3^m + I_4^m} \right) \quad (30)$$

3.2 Ergodic spectral efficiency in presence of LS channel estimation

In this case, the numerator in (24) is calculated from the following equality:

$$\begin{aligned} \mathbb{E} \left[\left(\hat{\mathbf{g}}_k^{ls} \right)^H \hat{\mathbf{g}}_k^m \right]^2 &= \text{Tr} \left\{ \mathbf{R}_k^2 \right\} + \mathbf{m}_k^H \mathbf{S}_k \mathbf{m}_k \\ &+ \mathbf{h}_k^H \mathbf{U}_k \mathbf{h}_k + \left| \text{Tr} \left\{ \mathbf{R}_k \right\} + \mathbf{h}_k^H \mathbf{m}_k \right|^2 \end{aligned} \quad (31)$$

Proof: First, express $\hat{\mathbf{g}}_k^m$ in terms of $\hat{\mathbf{g}}_k^l$. Then, use Lemma 3 in Appendix 7.2. The complete proof is provided in Appendix 7.4. \square

In order to evaluate the expectations in denominator, we define $I_n^{ls} \triangleq \mathbb{E}[I_n]$ for $n = 1, 2, 3, 4$.

1.

$$I_1^{ls} = \sum_{i \neq k} p_{li} \text{Tr} \left\{ \left(\mathbf{S}_k + \mathbf{m}_k \mathbf{m}_k^H \right) \left(\mathbf{U}_i + \mathbf{m}_i \mathbf{m}_i^H \right) \right\} \quad (32)$$

Proof: The proof has the same procedure for (26), except that \hat{g}_k^m is replaced with \hat{g}_k^{ls} . Consequently, the \mathbf{m}_k and \mathbf{U}_k are replaced with \mathbf{h}_k and \mathbf{S}_k , respectively. \square

2.

$$I_2^{ls} = \sum_{i=1}^K p_{li} \text{Tr} \left\{ \mathbf{V}_i \left(\mathbf{S}_k + \mathbf{m}_k \mathbf{m}_k^H \right) \right\} \quad (33)$$

Proof: Equation (33) can be verified by substituting $\mathbf{E}[(\hat{g}_k^{ls})^H \mathbf{V}_i \hat{g}_k^{ls}]$ in $\mathbf{E}[I_2]$, which is obtained by substituting $\mathbf{x} = \hat{g}_k^{ls}$, $\mathbf{m} = \mathbf{h}_k$, $\Sigma = \mathbf{S}_k$ and $\mathbf{A} = \mathbf{V}_i$ in Lemma 2 in Appendix 7.1. \square

3.

$$I_3^{ls} = \sum_{j \neq l} \sum_{i=1}^K p_{ji} \text{Tr} \left\{ \left(\mathbf{R}_{lji} + \mathbf{m}_{lji} \mathbf{m}_{lji}^H \right) \left(\mathbf{S}_k + \mathbf{h}_k \mathbf{h}_k^H \right) \right\} \quad (34)$$

Proof: It is identical to equation (28) proof except by replacing \mathbf{m}_k and \mathbf{U}_k with \mathbf{h}_k and \mathbf{S}_k , respectively. \square

4.

$$I_4^{ls} = \sigma_n^2 \left(\text{Tr} \{ \mathbf{S}_k \} + \|\mathbf{h}_k\|^2 \right). \quad (35)$$

Proof: Equation (35) is derived by substituting $\mathbf{x} = \hat{g}_k^{ls}$, $\mathbf{m} = \mathbf{h}_k$ and $\Sigma = \mathbf{S}_k$ in equation (47) of Appendix 7.1. \square

Therefore the ergodic SE of the k th user ($\bar{\eta}_k^{ls}$) in presence of LS channel estimation is approximated as

$$\bar{\eta}_k^{ls} = \gamma \log_2 \left(1 + \frac{p_{lk} \mathbf{E} \left[\left(\hat{g}_k^{ls} \right)^H \hat{g}_k^m \right]^2}{I_1^{ls} + I_2^{ls} + I_3^{ls} + I_4^{ls}} \right) \quad (36)$$

4 Numerical Results

In this section approximations in (30) and (36) are compared with Monte Carlo simulation results by using (17) for 100 channel realizations. They are also compared with [22] lower bounds. The SE curves related to their work are obtained by running their MATLAB functions. In all multi-cell simulations, a system with $L = 16$ cells is considered as in Fig. 3. It is assumed that $K = 10$ users are serviced in each cell.

4.1 Parameters

It is assumed that each BS is placed in the middle of the corresponding cell. Users are located randomly within a radius of 35 m to 250 m from BS in each cell. As mentioned in Section 2, \mathbf{R}_{ljk} depends on non-LOS large scale fading multiples (β_{ljk}^{NLOS}) and \mathbf{m}_{ljk} on LOS large scale fading multiples (β_{ljk}^{LOS}). If a strong LOS component exists then

$$\beta_{ljk}^{LOS} = \frac{\kappa_{ljk}}{1 + \kappa_{ljk}} \beta_{ljk} \quad (37)$$

$$\beta_{ljk}^{NLOS} = \frac{1}{1 + \kappa_{ljk}} \beta_{ljk} \quad (38)$$

where β_{ljk} (total large scale fading multiple) and κ_{ljk} (Rician factor) are defined as follows:

$$\beta_{ljk} [\text{dB}] = -30.18 - 26 \log_{10} (r_{ljk}) + z_{ljk}, z_{ljk} \sim N(0, 16) \quad (39)$$

Cell 4	Cell 8	Cell 12	Cell 16
Cell 3	Cell 7	Cell 11	Cell 15
Cell 2	Cell 6	Cell 10	Cell 14
Cell 1	Cell 5	Cell 9	Cell 13

Fig. 3: Configuration of $L = 16$ multi-cell system in simulations

$$\kappa_{ljk} [\text{dB}] = 13 - 0.03r_{ljk} \quad (40)$$

where r_{ljk} is the distance between the k th user in j th cell and BS in the l th cell and z_{ljk} is a related shadowing factor.

Some channels may have only non-LOS components, especially when there is a large distance between user and BS. If no LOS exists, then $\beta_{ljk}^{LOS} = 0$ and $\beta_{ljk}^{NLOS} = \beta_{ljk}$. In this case, we have:

$$\beta_{ljk} [\text{dB}] = -34.53 - 38 \log_{10} (r_{ljk}) + z_{ljk}, z_{ljk} \sim N(0, 100) \quad (41)$$

LOS existence depends on r_{ljk} . In the assumed model, no LOS exists for $r_{ljk} \geq 300$ m, and in other cases, it exists with the probability of $1 - r_{ljk}/300$. The s th element of \mathbf{m}_{ljk} is modelled as [27]

$$[\mathbf{m}_{ljk}]_s = \sqrt{\beta_{ljk}^{LOS}} \exp \left(J\pi(s-1) \sin(\theta_{ljk}) \right) \quad (42)$$

where $J \triangleq \sqrt{-1}$ and θ_{ljk} denotes the angle of arrival at l th BS from k th user in j th cell. Note that in this model, the antenna spacing is assumed to be half wavelength. The (s, t) th element of \mathbf{R}_{ljk} is presented as [28]:

$$\begin{aligned} [\mathbf{R}_{ljk}]_{s,t} &= \beta_{ljk}^{NLOS} \exp \left(J\pi(s-t) \sin(\theta_{ljk}) \right) \\ &\times \exp \left(-\frac{\sigma_\theta^2}{2} \left(\pi(s-t) \cos(\theta_{ljk}) \right)^2 \right) \end{aligned} \quad (43)$$

where σ_θ^2 is the angular standard deviation. For the uncorrelated channel, its covariance is considered as

$$\mathbf{R}_{ljk} = \beta_{ljk}^{NLOS} \mathbf{I} \quad (44)$$

The data and pilot symbol powers (p_{lk} and q_{lk}) are assumed to be different for all l and k in our calculations however for more simplicity we assume $p_{lk} = q_{lk}$ in all simulations. These values are chosen such that $p_{lk} \beta_{llk}$ is equal to a constant for all k . Moreover, the maximum value of p_{lk} is 10 dBm in each cell. Orthogonal pilot sequences are generated by using discrete Fourier transform (DFT) basis i.e.

$$[\boldsymbol{\phi}_k]_s = \exp \left(\frac{j2\pi(k-1)(s-1)}{\tau_p} \right). \quad (45)$$

Some of mentioned parameters and their values are listed in Table 1.

Table 1 Simulation Parameters

Parameter	Value
Number of Channel Realizations	100
Number of Symbols in a Coherence Block ($\tau_u + \tau_p$)	200
Number of Each User's Pilot Symbols (τ_p)	10
Noise Power (σ_n^2)	-94 dBm
Maximum User Transmitted Power	10 dBm
Angle of Arrival (θ_{ljk})	$\theta_{ljk} \sim \mathbb{U}(0, 2\pi)$
Angular Standard Deviation (σ_θ^2)	10°

4.2 Results

In Fig. 4a our proposed SE is compared with Monte Carlo simulation results and also with lower bounds in [22] for a multi-cell massive MIMO system with correlated Rician channel. Our approximation and simulation results are close to each other for both LS and MMSE channel estimators. It is seen that our SE is higher than the lower bound in [22].

SE of a single cell system is provided in Fig. 4b. No pilot contamination and inter-cell interference exist in the assumed system. It is seen that more SE can be achieved in a single cell system compared to the multi-cell system because only intra-cell interference exists. The difference between corresponding curves in Fig. 4a and 4b is higher for the LS channel estimation case. It is concluded that the LS estimator is more sensitive to pilot contamination than MMSE.

In Fig. 4c performance result for correlated Rayleigh channel is considered, where m_{ljk} is zero. In this case, non-LOS large scale fading is the same as that in the channel model of Fig. 4a. This leads to a decrease in both signal and interference powers. In Fig. 4c less SE is seen than in Fig. 4a. It can be concluded that in this case, signal power is decreased more than interference.

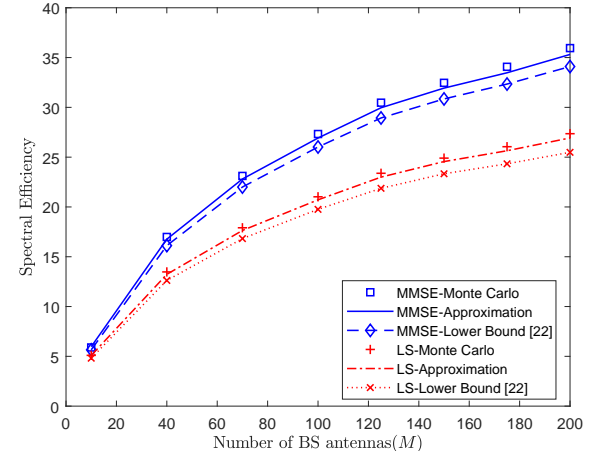
Fig. 5a shows SE performance comparison for both correlated and uncorrelated Rician channel in the presence of LS and MMSE estimators. In this case, the correlated channel has higher SE than uncorrelated. However, in other simulations for a highly correlated channel, SE is much lower than the corresponding curves in this Figure.

In Fig. 5b, the same comparison is done for the Rayleigh channel. Here, higher SE is seen for MMSE estimation in a correlated channel. For LS estimation, SE of the uncorrelated channel is higher than correlated at the high number of antennas for both approximation and Monte Carlo curves. However, at the low number of antennas, it is vice versa for approximation curves. Monte Carlo curves have the same SE at the low number of antennas. It is also seen that LS and MMSE estimators have the same SE in uncorrelated Rayleigh channel as well as the lower bounds [22] (as in Fig. 6). That is because here \hat{g}_k^m is a scale of \hat{g}_k^{ls} and this scale does not affect SINR_k in both works.

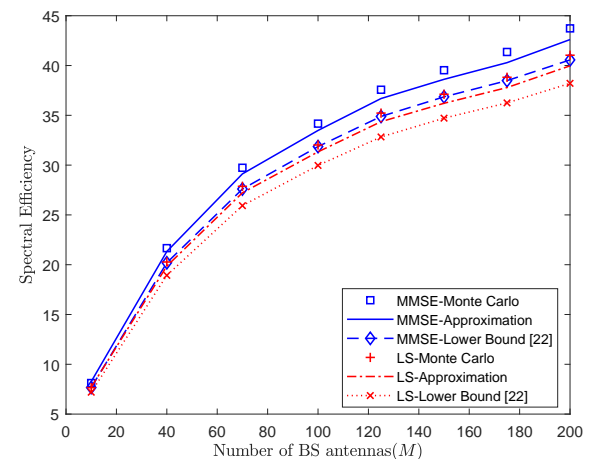
In all simulations, it is seen that the approximations in (30) and (36) are close enough to Monte Carlo simulation results of equation (17). They were also higher than lower bounds provided in [22]. By increasing the number of BS antennas, the gap between approximations and results of Monte Carlo simulation decreases. But it increases for the approximations and lower bounds.

5 Conclusion

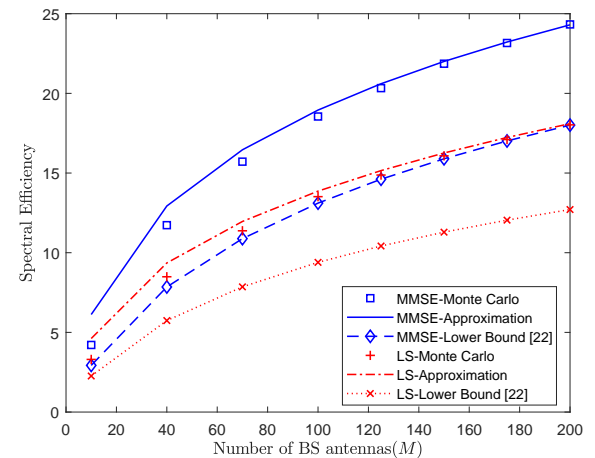
In this work, SE of multi-cell massive MIMO was investigated for MRC detector, LS and MMSE estimators in a correlated Rician channel. Since for LS estimator signal and interference parts are cross-correlated at detector output, SE analysis is more complicated than MMSE. Different from previous works in which part of the signal was subtracted and added to the interference part, we extracted the cross-correlated part of the interference with the signal completely and added it to the signal part. Closed form approximations of ergodic SE were derived for both LS and MMSE channel estimators. It was shown that our approximations are close to Monte Carlo simulation results at the high number of antennas. It was observed that our SE is higher than the lower bounds in earlier works. It was seen that MMSE channel estimation outperforms LS or they have the same SE in uncorrelated Rayleigh channel. In future work, we consider



(a) Multi-cell Rician Channel



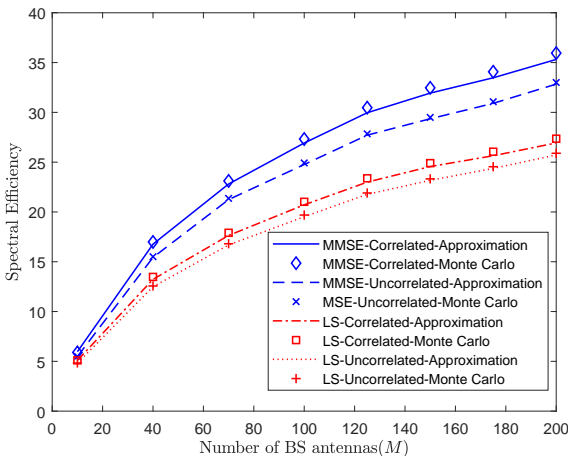
(b) Single-cell Rician Channel



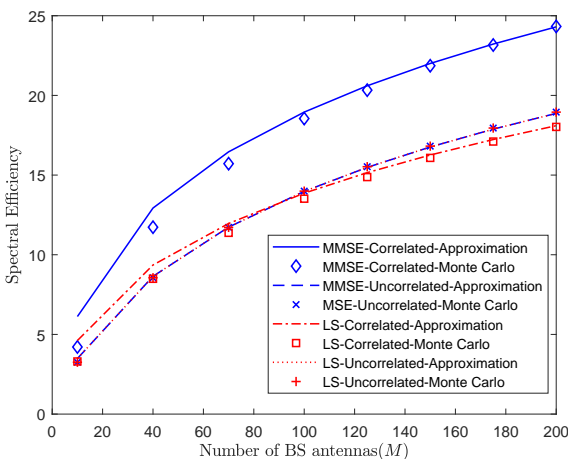
(c) Multi-cell Rayleigh Channel

Fig. 4: Comparison of our SE approximation with Monte Carlo simulation and lower bounds in a system with correlated channel for MRC detector and MMSE and LS channel estimations

applying our approach to ZF or MMSE detector to obtain the instantaneous SE. Moreover, we investigate ergodic SE approximation of these detectors.



(a) Rician Channel



(b) Rayleigh Channel

Fig. 5: SE Comparison of correlated and uncorrelated channel in a multi-cell system for MRC detection and LS and MMSE channel estimation

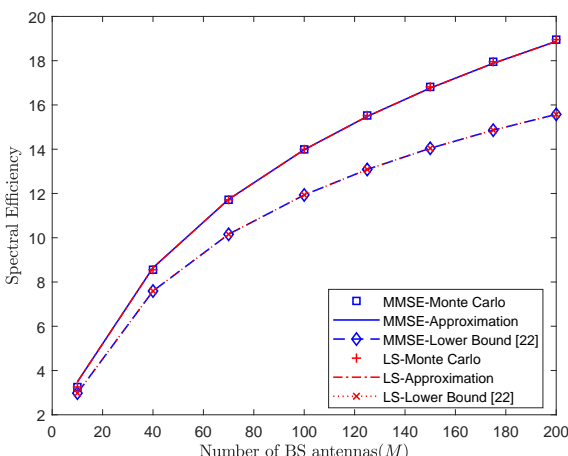


Fig. 6: Comparison of our SE approximation with Monte Carlo simulation and lower bounds in a multi-cell system with uncorrelated Rayleigh channel for MRC detector and MMSE and LS channel estimations

6 References

- 1 Andrews, J.G., Buzzi, S., Choi, W., Hanly, S.V., Lozano, A., Soong, A.C.K., et al.: 'What Will 5G Be?', *IEEE Journal on Selected Areas in Communications*, 2014, **32**, (6), pp. 1065–1082
- 2 Aražjo, D.C., Maksymuk, T., de Almeida, A.L.F., Maciel, T., Mota, J.C.M., Jo, M.: 'Massive MIMO: survey and future research topics', *IET Communications*, 2016, **10**, (15), pp. 1938–1946
- 3 Larsson, E.G., Edfors, O., Tufvesson, F., Marzetta, T.L.: 'Massive MIMO for next generation wireless systems', *IEEE Communications Magazine*, 2014, **52**, (2), pp. 186–195
- 4 Marzetta, T.L.: 'Noncooperative Cellular Wireless with Unlimited Numbers of Base Station Antennas', *IEEE Transactions on Wireless Communications*, 2010, **9**, (11), pp. 3590–3600
- 5 Marzetta, T.L.: 'Massive MIMO: An Introduction', *Bell Labs Technical Journal*, 2015, **20**, pp. 11–22
- 6 Björnson, E., Larsson, E.G., Marzetta, T.L.: 'Massive MIMO: ten myths and one critical question', *IEEE Communications Magazine*, 2016, **54**, (2), pp. 114–123
- 7 Alwakeel, A.S., Mehana, A.M.H.: 'Achievable Rates in Uplink Massive MIMO Systems With Pilot Hopping', *IEEE Transactions on Communications*, 2017, **65**, (10), pp. 4232–4246
- 8 Ngo, H.Q., Larsson, E.G., Marzetta, T.L.: 'Energy and Spectral Efficiency of Very Large Multiuser MIMO Systems', *IEEE Transactions on Communications*, 2013, **61**, (4), pp. 1436–1449
- 9 Lu, S., Wang, Z.: 'Achievable rates of uplink multiuser massive MIMO systems with estimated channels'. In: 2014 IEEE Global Communications Conference. (, 2014, pp. 3772–3777
- 10 Wang, X., Wang, Y., Ma, S.: 'Upper Bound on Uplink Sum Rate for Multi-Cell Massive MU-MIMO Systems With ZF Receivers', *IEEE Wireless Communications Letters*, 2017, **6**, (2), pp. 250–253
- 11 Yao, R., Li, T., Liu, Y., Zuo, X., Liu, H.: 'Analytical Approximation of the Channel Rate for Massive MIMO System With Large But Finite Number of Antennas', *IEEE Access*, 2018, **6**, pp. 6496–6504
- 12 Kazemi, M., Aghaeinia, H.: 'Approximate ergodic capacity of multiuser massive multiple input multiple output in a Rayleigh fading uplink channel with variance profile', *IET Communications*, 2015, **9**, pp. 844–852(8)
- 13 Younas, T., Li, J., Arshad, J., Tulu, M.M.: 'Performance analysis of improved ZF algorithm for massive MIMO in uplink', *Electronics Letters*, 2017, **53**, (23), pp. 1554–1556
- 14 Xing, P., Liu, J., Zhai, C., Wang, X., Zheng, L.: 'Spectral efficiency of the in-band full-duplex massive multi-user multiple-input multiple-output system', *IET Communications*, 2017, **11**, (4), pp. 490–498
- 15 Yang, H., Marzetta, T.L.: 'Performance of Conjugate and Zero-Forcing Beamforming in Large-Scale Antenna Systems', *IEEE Journal on Selected Areas in Communications*, 2013, **31**, (2), pp. 172–179
- 16 Khansefid, A., Minn, H.: 'Achievable Downlink Rates of MRC and ZF Precoders in Massive MIMO With Uplink and Downlink Pilot Contamination', *IEEE Transactions on Communications*, 2015, **63**, (12), pp. 4849–4864
- 17 Jiang, Z., Molisch, A.F., Caire, G., Niu, Z.: 'Achievable Rates of FDD Massive MIMO Systems With Spatial Channel Correlation', *IEEE Transactions on Wireless Communications*, 2015, **14**, (5), pp. 2868–2882
- 18 Zhang, X., Wu, S., Yu, S., Liu, J.: 'Spectral efficiency of massive MIMO networks with pilot contamination and channel covariance matrix estimation', *IET Communications*, 2019, **13**, (1), pp. 59–65
- 19 Nyarko, J.K.N., Xie, J., Yao, R., Wang, Y., Wang, L.: 'Analytical approximation of ZF Ricean rate in massive MIMO channels', *Electronics Letters*, 2019, **55**, (4), pp. 224–226
- 20 Tataria, H., Smith, P.J., Greenstein, L.J., Dmochowski, P.A., Matthaiou, M.: 'Impact of Line-of-Sight and Unequal Spatial Correlation on Uplink MU-MIMO Systems', *IEEE Wireless Communications Letters*, 2017, **6**, (5), pp. 634–637
- 21 Liu, J., Dai, J., Wang, J., Zhao, J., Cheng, C.: 'Achievable Rates for Full-Duplex Massive MIMO Systems Over Rician Fading Channels', *IEEE Access*, 2018, **6**, pp. 30208–30216
- 22 AÜ. AÜzdogan, Björnson, E., Larsson, E.G.: 'Massive MIMO With Spatially Correlated Rician Fading Channels', *IEEE Transactions on Communications*, 2019, **67**, (5), pp. 3234–3250
- 23 Kazemi, M., Aghaeinia, H.: 'A lower bound on achievable rate of MRT pre-coding in multicell multiuser massive MIMO networks with Rician flat fading', *International Journal of Communication Systems*, 2016, **29**, (18), pp. 2632–2649. Available from: <https://onlinelibrary.wiley.com/doi/abs/10.1002/dac.3134>
- 24 Nyarko, J.K.N., Xie, J., Yao, R., Wang, Y., Wang, L.: 'Accurate Approximation of ZF Massive MIMO Channel Rate With a Finite Antenna Over Ricean Fading Channel', *IEEE Access*, 2018, **6**, pp. 65803–65812
- 25 Kay, S.M.: 'Fundamentals of statistical signal processing, volume I: estimation theory'. (Prentice Hall, 1993)
- 26 Zhang, Q., Jin, S., Wong, K.K., Zhu, H., Matthaiou, M.: 'Power Scaling of Uplink Massive MIMO Systems With Arbitrary-Rank Channel Means', *IEEE Journal of Selected Topics in Signal Processing*, 2014, **8**, (5), pp. 966–981
- 27 Björnson, E., Hoydis, J., Sanguinetti, L.: 'Massive MIMO Networks: Spectral, Energy, and Hardware Efficiency', *Foundations and Trends® in Signal Processing*, 2017, **11**, (3–4), pp. 154–655. Available from: <http://dx.doi.org/10.1561/2000000093>
- 28 3GPP. 'Further advancements for E-UTRA physical layer aspects'. (3rd Generation Partnership Project (3GPP), 2010. 36.814. version 9.0.0. Available from: <https://portal.3gpp.org/desktopmodules/Specifications/SpecificationDetails.aspx?specificationId=2493>
- 29 Brookes, M.: 'The Matrix Reference Manual', Available: <http://www.eeimperial.ac.uk/hp/staff/dmb/matrix/introhtml>, 2011,

7 Appendix

7.1 Quadratic Expectations of a Complex Normal Vector

Lemma 2. If $\mathbf{x} \sim \mathbb{C}N(\mathbf{m}, \Sigma)$ then for any matrix A we have

$$\mathbb{E}[\mathbf{x}^H A \mathbf{x}] = \text{Tr}\{A(\Sigma + \mathbf{m}\mathbf{m}^H)\} \quad (46)$$

In an especial case, that $A = \mathbf{I}$, (46) is simplified as

$$\mathbb{E}[\|\mathbf{x}\|^2] = \text{Tr}\{\Sigma\} + \|\mathbf{m}\|^2 \quad (47)$$

Another quadratic expectation used in our derivations is

$$\mathbb{E}[\mathbf{x}\mathbf{x}^H] = \Sigma + \mathbf{m}\mathbf{m}^H \quad (48)$$

7.2 Quartic Expectation of a Complex Normal Vector

Lemma 3. If $\mathbf{x} \sim \mathbb{C}N(\mathbf{m}, \Sigma)$ then for any non-zeros matrices A, B, C, D and arbitrary vectors $\mathbf{a}, \mathbf{b}, \mathbf{c}, \mathbf{d}$ the following expectation holds [29]

$$\begin{aligned} \mathbb{E}[(\mathbf{Ax} + \mathbf{a})^H (\mathbf{Bx} + \mathbf{b})(\mathbf{Cx} + \mathbf{c})^H (\mathbf{Dx} + \mathbf{d})] = \\ \text{Tr}\{A^H B \Sigma C^H D \Sigma\} + (\mathbf{Cm} + \mathbf{c})^H D \Sigma A^H (\mathbf{Bm} + \mathbf{b}) \\ + (\mathbf{Am} + \mathbf{a})^H B \Sigma C^H (\mathbf{Dm} + \mathbf{d}) \\ + \left(\text{Tr}\{B \Sigma A^H\} + (\mathbf{Am} + \mathbf{a})^H (\mathbf{Bm} + \mathbf{b})\right) \\ \times \left(\text{Tr}\{D \Sigma C^H\} + (\mathbf{Cm} + \mathbf{c})^H (\mathbf{Dm} + \mathbf{d})\right) \end{aligned} \quad (49)$$

For a specific case that $A = B = C = D = \mathbf{I}$ and $\mathbf{a} = \mathbf{b} = \mathbf{c} = \mathbf{d} = \mathbf{0}$, it follows that

$$\mathbb{E}[\|\mathbf{x}\|^4] = \text{Tr}\{\Sigma^2\} + 2\mathbf{m}^H \Sigma \mathbf{m} + (\text{Tr}\{\Sigma\} + \|\mathbf{m}\|^2)^2 \quad (50)$$

7.3 Equation (26) proof

First, $\mathbb{E}[(\hat{\mathbf{g}}_k^m)^H \hat{\mathbf{g}}_i^m]^2$ is derived for specific i and k such that $i \neq k$. For this purpose, the inside expression is modified. The expression $[(\hat{\mathbf{g}}_k^m)^H \hat{\mathbf{g}}_i^m]^2$ is scalar and equals its trace. By using the commutative property of trace we have

$$\left|(\hat{\mathbf{g}}_k^m)^H \hat{\mathbf{g}}_i^m\right|^2 = \text{Tr}\{(\hat{\mathbf{g}}_k^m)^H \hat{\mathbf{g}}_i^m (\hat{\mathbf{g}}_i^m)^H \hat{\mathbf{g}}_k^m\} \quad (51)$$

Since expectation and trace are both linear operators, changing their order does not change the result. Hence, we apply expectation to expression inside of trace (51). By using independence of $\hat{\mathbf{g}}_i^m, \hat{\mathbf{g}}_k^m$ and also using (48), we have

$$\mathbb{E}\left[\left|(\hat{\mathbf{g}}_k^m)^H \hat{\mathbf{g}}_i^m\right|^2\right] = \text{Tr}\{(\mathbf{U}_k + \mathbf{m}_k \mathbf{m}_k^H)(\mathbf{U}_i + \mathbf{m}_i \mathbf{m}_i^H)\} \quad (52)$$

Finally, the equation (26) is derived as follows

$$\begin{aligned} I_1^m &= \sum_{i \neq k} p_{li} \mathbb{E}\left[\left|(\hat{\mathbf{g}}_k^m)^H \hat{\mathbf{g}}_i^m\right|^2\right] \\ &= \sum_{i \neq k} p_{li} \text{Tr}\{(\mathbf{U}_k + \mathbf{m}_k \mathbf{m}_k^H)(\mathbf{U}_i + \mathbf{m}_i \mathbf{m}_i^H)\} \end{aligned} \quad (53)$$

7.4 Equation (31) Proof

For calculating $\mathbb{E}[(\hat{\mathbf{g}}_k^m)^H \hat{\mathbf{g}}_k^m]^2$, MMSE estimation ($\hat{\mathbf{g}}_k^m$) is rewritten in terms of $\hat{\mathbf{g}}_k^{ls}$ as follows:

$$\hat{\mathbf{g}}_k^m = \mathbf{F}_k \hat{\mathbf{g}}_k^{ls} + \mathbf{f}_k \quad (54)$$

where

$$\mathbf{F}_k = \mathbf{R}_k \mathbf{S}_k^{-1} \quad (55)$$

$$\mathbf{f}_k = \mathbf{m}_k - \mathbf{F}_k \mathbf{h}_k \quad (56)$$

Now equation (49) can be used to calculate $\mathbb{E}[(\hat{\mathbf{g}}_k^m)^H \hat{\mathbf{g}}_k^m]^2$ by substituting $\mathbf{x} = \hat{\mathbf{g}}_k^{ls}, \mathbf{m} = \mathbf{h}_k, \Sigma = \mathbf{S}_k, \mathbf{A} = \mathbf{D} = \mathbf{I}, \mathbf{B} = \mathbf{C} = \mathbf{F}_k, \mathbf{a} = \mathbf{d} = \mathbf{0}$ and $\mathbf{b} = \mathbf{c} = \mathbf{f}_k$. Applying the substitution to the right side of (49) leads to a sum of four complicated terms which are simplified as follows:

- First, the expression $\mathbf{A}^H \mathbf{B} \Sigma \mathbf{C}^H \mathbf{D} \Sigma$ which equals $\mathbf{F}_k \mathbf{S}_k \mathbf{F}_k^H \mathbf{S}_k$ is simplified as $\mathbf{R}_k \mathbf{S}_k^{-1} \mathbf{R}_k \mathbf{S}_k$. This is the result of applying (55) and considering that \mathbf{R}_k and \mathbf{S}_k are self-adjoint matrices. The product $\mathbf{S}_k^{-1} \mathbf{R}_k \mathbf{S}_k$ is simplified as $(\mathbf{R}_k^{-1} \mathbf{S}_k)^{-1} \mathbf{S}_k = \mathbf{R}_k$. It follows that $\mathbf{A}^H \mathbf{B} \Sigma \mathbf{C}^H \mathbf{D} \Sigma = \mathbf{R}_k^2$ in this case.
- The second expression $(\mathbf{Cm} + \mathbf{c})^H \mathbf{D} \Sigma \mathbf{A}^H (\mathbf{Bm} + \mathbf{b})$ is equal to $(\mathbf{F}_k \mathbf{h}_k + \mathbf{f}_k)^H \mathbf{S}_k (\mathbf{F}_k \mathbf{h}_k + \mathbf{f}_k)$. We conclude from (56) that $\mathbf{F}_k \mathbf{h}_k + \mathbf{f}_k = \mathbf{m}_k$. It follows that $(\mathbf{Cm} + \mathbf{c})^H \mathbf{D} \Sigma \mathbf{A}^H (\mathbf{Bm} + \mathbf{b}) = \mathbf{m}_k^H \mathbf{S}_k \mathbf{m}_k$.
- We have for the third expression: $(\mathbf{Am} + \mathbf{a})^H \mathbf{B} \Sigma \mathbf{C}^H (\mathbf{Dm} + \mathbf{d}) = \mathbf{h}_k^H \mathbf{F}_k \mathbf{S}_k \mathbf{F}_k \mathbf{h}_k$. The product $\mathbf{F}_k \mathbf{S}_k \mathbf{F}_k$ is equal to $\mathbf{R}_k \mathbf{S}_k^{-1} \mathbf{R}_k$. According to (12), it equals \mathbf{U}_k . Consequently, it is concluded that $(\mathbf{Am} + \mathbf{a})^H \mathbf{B} \Sigma \mathbf{C}^H (\mathbf{Dm} + \mathbf{d}) = \mathbf{h}_k^H \mathbf{U}_k \mathbf{h}_k$.
- The fourth expression is a product of two terms that each contains three parts. From previous expression derivation: $\mathbf{Bm} + \mathbf{b} = \mathbf{Cm} + \mathbf{c} = \mathbf{m}_k$, $\mathbf{Am} + \mathbf{a} = \mathbf{Dm} + \mathbf{d} = \mathbf{h}_k$ and $\mathbf{B} \Sigma \mathbf{A}^H = (\mathbf{D} \Sigma \mathbf{C}^H)^H$. Hence, we have: $\text{Tr}\{\mathbf{B} \Sigma \mathbf{A}^H\} = \text{Tr}\{\mathbf{D} \Sigma \mathbf{C}^H\}^*$ (The notation $*$ denotes complex conjugate). Therefore, the fourth expression is a product of a term with its complex conjugate. We also have: $\mathbf{B} \Sigma \mathbf{A}^H = \mathbf{F}_k \mathbf{S}_k = \mathbf{R}_k$. Consequently, the fourth expression in (49) is $|\text{Tr}\{\mathbf{R}_k\} + \mathbf{h}_k^H \mathbf{m}_k|^2$.

Finally, inserting all terms in (49), gives (31).